Phase transition at H_{c1} for superconducting Nb and V

J. J. Wollan,* K. W. Haas, John R. Clem, and D. K. Finnemore

Ames Laboratory U. S. Atomic Energy Commission and Department of Physics, Iowa State University, Ames, Iowa 50010

(Received 20 May 1974)

Magnetization curves for V and Nb have been studied to look for a first-order transition at H_{c1} and to determine the temperature interval in which the interaction between quantized vortices is attractive. Both the Nb sample with resistivity ratio of $\Gamma \approx 1000$ and the V sample with $\Gamma \approx 1500$ show a very sharp rise in magnetic induction at H_{c1} which is reminiscent of a first-order transition. The values of vortex spacing derived from the magnitude of this abrupt rise agree well with the decoration technique at 1.2 K and the neutron-diffraction technique at 4 K. As the temperature increases, the magnetic-induction curves near H_{c1} retain the same shape for all temperatures up to reduced temperatures above 0.95. Hence there is no evidence in the magnetization data for a changeover from an attractive to a repulsive interaction in this temperature range. The detailed shape of the phase-transition curves near H_{c1} agrees fairly well with model-calculations which include only bulk pinning.

INTRODUCTION

The interaction between quantized vortices in superconductors[1-7] can be either attractive or repulsive, depending on the relative magnitudes of the penetration depth λ and the coherence distance ξ. For dirty materials, where $\xi \ll \lambda$ and the local theory applies,[8] one expects a repulsive interaction between vortices and a second-order transition at H_{c1}. For relatively clean materials where $\xi \approx \lambda$ and nonlocal effects are important, one expects an attractive interaction[1] between vortices and a first-order transition at H_{c1}. As yet, there is no complete theory for these effects, but preliminary calculations by Dichtel,[9] by Kramer,[7] and by Leung and Jacobs[5] and measurements by Auer and Ullmaier[10] indicate that the attractive interaction occurs for κ values in the range between about 0.5 and 1.2, where κ is defined in terms of the ratio of the upper critical field H_{c2} and the thermodynamic critical field H_c as $\kappa = H_{c2}/\sqrt{2}H_c$.

The first clear-cut evidence for an attractive interaction between vortices in low-κ materials was the decoration experiments of Essmann[11] and Träuble at 1.2 K. These experiments clearly showed the coexistence of Meissner and vortex domains in the sample, as would be expected for an attractive interaction. In addition, neutron-diffraction studies by Schelten and co-workers[3] at 4.2 K also showed that the vortex lattice at H_{c1} grows with constant lattice spacing as the volume fills with vortices. Hence, for the case of Nb, it is rather certain that there is an attractive interaction at least at temperatures below 4.2 K.

At temperatures very close to T_c, one expects that all samples should show a regime where the Ginzburg-Landau theory[8] applies. Hence materials which show an attractive interaction at low temperature must have a phase boundary, which separates the low-temperature attractive region from the high-temperature repulsive region, similar to the phase boundary calculated by Kramer.[6] Indeed, Auer and Ullmaier[10] have made an experimental study of this phase boundary in TaN alloys and find a boundary between the repulsive and attractive regimes. However, they find quantitative differences from the theory,[6] in that the attractive-to-repulsive interaction phase boundary occurs at higher temperatures than the calculations predict. In addition, magnetization data by Kumpf[4] and by Finnemore, Stromberg, and Swenson[12] for Nb indicate that in this metal the phase boundary may be at a substantially higher temperature than predicted.

There is little doubt that an attractive interaction exists in Nb at temperatures below 4.2 K from the decoration[2] and neutron studies.[3] Because these measurements are difficult to make near T_c, it would not be suitable to look for the phase boundary by these techniques. Magnetization measurements, on the other hand, can be easily made over the entire temperature range, so this method was chosen to look for the phase boundary. There may be some ambiguity about the determination of the flux-line spacing d_0 from the magnetization curves because the samples are not ideal in behavior. The decoration and neutron studies, however, can be used to verify the interpretation at low temperatures and then one can assume that this interpretation applies over the entire temperature range. The primary purpose of this work is to study the phase transition at H_{c1} for both Nb and V and to look for a region of repulsive interaction between vortices near T_c.

PHASE TRANSITION AT H_{c1}

All studies of the phase transition at H_{c1} must contend with basic irreversibilities in the transi-

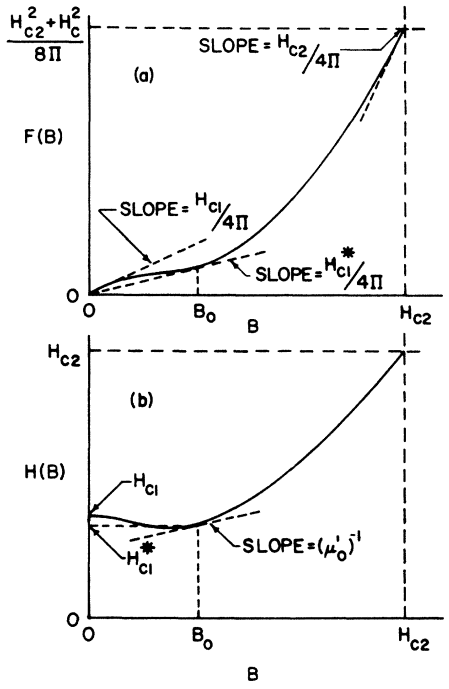

FIG. 1. (a) A sketch of the Helmholtz free-energy density as a function of B for an attractive vortex-vortex interaction. (b) A sketch of the field $H(B) = 4\pi\,\partial F(B)/\partial B$ as a function of B.

tion which arise because there are free-energy barriers which inhibit the entry of fluxoids. A major contributing factor, of course, is the fundamental free-energy barrier caused by the image forces on the vortices at a vacuum-superconductor interface.[8] This effect alone guarantees hysteresis even if the surface is perfect. In addition there may be imperfections which cause bulk and additional surface pinning effects. Hence one expects on theoretical grounds to find irreversibilities, and indeed they are observed for every sample we have measured. The magnitude of the hysteresis is typically a few percent of H_{c1} for the best Nb and V samples.

Another complication which is relevant to the study of first-order transitions at H_{c1} is the observation that the B vs H curves for long, thin samples of type-II superconductors never rise as fast as would be predicted from the geometrical demagnetizing factor. The work of French[13] for Nb shows the steepest rise at 200 G/Oe, but this is about a factor of 2 less steep than the slope predicted from the demagnetizing factor. The work of Auer and Ullmaier[10] on TaN alloys shows a slope of about 60 G/Oe, but this is at least a factor of 5 less than predicted from the demagnetizing factor. In fact, all published data to date for type-II materials with a very small demagnetizing factor show this smaller slope, whereas type-I materials such as Sn, In, and Hg (Ref. 14) show B vs H curves which rise at the demagnetizing slope. There seems to be a fundamental difference when quantized vortices are involved. As we shall show below, a small amount of bulk pinning can account for the smaller observed slopes at H_{c1}.

In order to demonstrate how this can occur, let us first consider the expected behavior of an ideal (pinning-free) infinite cylinder of radius R in thermodynamic equilibrium. When the vortex-vortex interaction is attractive at low flux density, the Helmholtz free-energy density $F(B)$, relative to the Meissner phase, associated with interacting quantized vortices in a triangular lattice with flux density B, behaves qualitatively as shown in Fig. 1(a). The value of F at H_{c2} is $(H_{c2}^2 + H_c^2)/8\pi$. Because the magnetic field in the specimen interior, sketched in Fig. 1(b), is defined as $H(B) = 4\pi\partial F(B)/\partial B$, the slope of the curve of F vs B is equal to $H_{c1}/4\pi$ at $B = 0$ and $H_{c2}/4\pi$ at $B = H_{c2}$. The pressure required to hold the vortices in equilibrium is[8] $p(B) = BH(B)/4\pi - F(B) = -G(B)$, where G is the Gibbs free-energy density relative to the Meissner phase. With increasing B, the Gibbs free-energy first becomes negative, indicating that the mixed state has become energetically favored over the Meissner phase, when $B = B_0$, where B_0 is the solution of $F(B) = B\partial F(B)/\partial B$. We denote the magnetic field at which this occurs as $H_{c1}^* = H(B_0)$. Accordingly, the vortex pressure is positive when $B > B_0$, vanishes when $B = B_0$, and is negative for $0 < B < B_0$. As a function of the applied field H_a, the average flux density $\bar{B}$ in such a cylinder, assuming it can always remain in thermodynamic equilibrium, is zero when $0 < H_a < H_{c1}^*$, jumps discontinuously to B_0 at $H_a = H_{c1}^*$, then rises initially with slope $\mu_0' = [dH(B_0)/dB_0]^{-1}$ upon further increase of H_a, as shown by curve a in Fig. 2.

We now include the effects of bulk pinning, which we describe in terms of the critical-state model.[15] In a static flux-filled region, the $\vec{H}$ field obeys $\nabla \times \vec{H} = 4\pi\vec{J}/c$, where the magnitude of $\vec{J}$ is equal to the bulk critical current density $J_c(B)$. We shall assume that the specimen remains in thermodynamic equilibrium except for the effects of bulk pinning. As a magnetic field H_a is applied parallel to the cylinder axis, flux penetration begins at H_{c1}^*. Initially a flux front of flux density $B \approx B_0$ is formed around the perimeter of the cylinder. Within the flux-filled region, the field gradient is given by $\partial H/\partial\rho = 4\pi J_c(B)/c$, where ρ is the radial coordinate. In the field region $H \approx H_{c1}^*$, we assume, for simplicity, that the value of $J_c(B)$ remains nearly constant with the value $J_{c0} = J_c(B_0)$ and that $B \approx B_0 + \mu_0'(H - H_{c1}^*)$. Provided $H_{c1}^* < H_a < H_p = H_{c1}^* + \Delta H_p$, the flux density is easily found to be

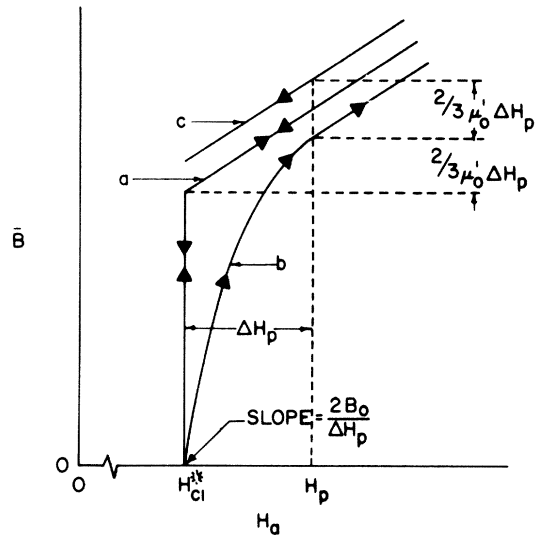

FIG. 2. Prediction of the critical-state bulk-pinning model for the value of the magnetic induction averaged over the entire sample $\bar{B}$, as a function of applied field H_a, in the vicinity of the lower critical field. Curve (a) shows the behavior for increasing H_a. Curve (c) shows the behavior for decreasing H_a. The magnitude of the hysteresis in $\bar{B}$ at H_p is given by $\Delta\bar{B}_p = 2\mu_0'\Delta H_p/3$.

$$B(\rho) = 0 , \qquad 0 < \rho < \rho_p$$

$$B(\rho) = B_0 + \mu_0'\Delta H_p(\rho - \rho_p)/R , \quad \rho_p < \rho < R$$

where $\Delta H_p = 4\pi J_{c0}R/c$ is the difference between the external and axial fields that can be supported by pinning;

$$\rho_p = R[1 - (H_a - H_{c1}^*)/\Delta H_p]$$

is the radius of penetration of the flux front; and $H_p = H_{c1}^* + \Delta H_p$ is the applied field at which the flux front first penetrates to the specimen axis. In this field range the *average* flux density (flux divided by specimen cross-sectional area) is found by integration to be

$$\bar{B} = B_0(2x - x^2) + \mu_0'\Delta H_p(x^2 - x^3/3) , \qquad (1)$$

where $x = (H_a - H_{c1}^*)/\Delta H_p$. When H_a exceeds H_p by a small amount and is increasing, the flux density is

$$B(\rho) = B_0 + \mu_0'(H_a - H_p) + \mu_0'\Delta H_p\rho/R$$

and the *average* flux density is

$$\bar{B} = B_0 + \mu_0'(H_a - H_{c1}^*) - \mu_0'\Delta H_p/3 .$$

Similarly, when H_a exceeds H_{c1}^* by a small amount and is *decreasing*, the flux density is

$$B(\rho) = B_0 + \mu_0'(H_a - H_{c1}^*) + \mu_0'\Delta H_p(1 - \rho/R)$$

and the average flux density is

$$\bar{B} = B_0 + \mu_0'(H_a - H_{c1}^*) + \mu_0'\Delta H_p/3 .$$

In summary, we expect bulk pinning to produce the following effects upon the behavior of $\bar{B}$ in an increasing applied field $H_a \sim H_{c1}^*$. We expect $\bar{B}$ to be zero when $0 < H_a < H_{c1}^*$, to rise sharply with initial slope $2B_0/\Delta H_p$ at H_{c1}^*, to then bend over and first assume the slope μ_0' when $H_a = H_p$, at which $B = B_0 + 2\mu_0'\Delta H_p/3$. These effects are shown in curve *b* in Fig. 2. For decreasing field, shown by curve *c* of Fig. 2, there will be hysteresis in the value of $\bar{B}$ of $2\mu_0'\Delta H_p/3$ at a field near H_p. The magnitude of this hysteresis, of course, can be directly tested by experiment.

EXPERIMENTAL

Sample preparation

A vanadium sample with a resistivity ratio ($\rho_{300}/\rho_{4.2}$) of 1500 was prepared in the form of a cylindrical rod by an electrotransport technique[16] which utilized very pure helium gas to suppress the vaporization at high temperatures. The rod was cut to a length of about 2.4 cm and the ends were mechanically polished to a hemispherical shape. It was then electropolished in a 6% perchloric acid in methanal solution to the final dimension of 2.5 cm long by 0.23 cm diameter. After a major portion of the vanadium magnetization data had been taken, the sample was further electropolished to reduce the demagnetizing factor. This left a slightly irregular shape which had a cross section that was roughly elliptical with a semimajor axis of 0.11 cm and a semiminor axis of 0.081 cm. The length was 2.1 cm.

The Nb data were taken on the same samples used for the surface superconductivity measurements[17] reported earlier, so a brief description will suffice here. The sample was outgassed near the melting point in a vacuum of 2×10^{-9} torr and sealed in a glass capillary under helium without exposure to air. After a series of magnetization measurements had been made, the capillary was opened and the sample was anodized in an H_2SO_4 solution at 20 V. The purpose of the anodization was to convert any surface layer of niobium monoxide into the pentoxide. The anodization made essentially no difference in the magnetization data.

Both the V and the Nb samples were composed of several single crystals which extended across the diameter of the specimen and had a length of about 1 to 3 times the diameter. The pickup coils used for the magnetization measurements were much smaller than the length of the sample to avoid end effects and normally they covered the region of two or three single crystals. For the case of V, the coil was centered on the largest single crystal, 0.48 cm long, but the coil was large enough that it was somewhat sensitive to the adjacent crystal.

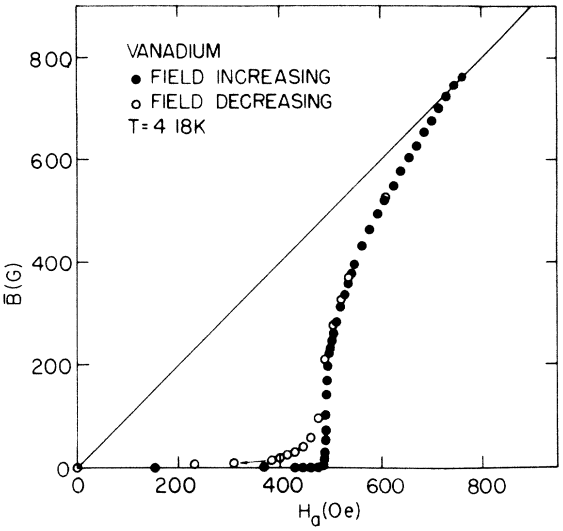

FIG. 3. Magnetic induction curve for the most reversible vanadium sample.

This center crystal had the [110] axis along the cylindrical axis and hence the applied field. The adjacent crystals were somewhat misaligned but they had the [110] axis within 7° of the magnetic field. For the Nb sample the diameter of the rod and the single crystals were somewhat smaller than for V, so no special effort was made to center the coils on a particular single crystal. X-ray analysis shows that most of the single crystals had the [100] close to the cylindrical axis (5–10 deg) but there was considerable variation.

Apparatus

Magnetization data for V and Nb were taken by two rather different means. For vanadium, the data were taken with a sample motion magnetometer similar to that used in the early Nb work.[12] The sample, which was located in the helium bath, was driven out of a pickup coil in a smooth stroke by a bellows-activated apparatus. Typical motion times would be a few tenths of a second. The thermal conductivity of He^4 above the λ point is rather poor, so a large copper shield surrounded the region of the sample to reduce the temperature gradients. A heater and sensing thermometer were mounted on this shield to control the temperature to 0.001 K. For the data reported here, the temperature drifted less than 0.001 K over the time required for a magnetization run (~1 h). Values of the temperature were determined from a germanium resistor (GR251) which had been calibrated previously from the vapor pressure[18] of He^4 and a constant-volume gas thermometer.[19] The temperature scale is essentially T-58.[18]

For Nb, magnetization data were taken with a field-stepping technique similar to that described by Cochran, Mapother, and Mould.[20] Coils 0.62-cm long, near the center of the sample, were used to detect changes in induction associated with a small step in the applied field. The time constant for changes in the field was a few milliseconds. In this apparatus the sample, pickup coils, and thermometer were isolated from the bath so that there was no difficulty regulating temperature to a few tenths of a millikelvin for any desired period. Values of the temperature were determined from a germanium thermometer which had been calibrated in the same experiment as GR251.

RESULTS AND DISCUSSION

Magnetic induction data for the most reversible vanadium sample are shown in Fig. 3. In this figure the value of B averaged over the entire sample $\bar{B}$ is plotted versus H. For the increasing field data (solid circles), $\bar{B}$ rises very rapidly until it is about 40% of H_{c1} and then slowly bends over to meet the $B=H$ line at H_{c2}. For the decreasing field data (open circles), $\bar{B}$ lies slightly higher than the increasing field data but the sample shows only a few percent hysteresis and no measurable trapped flux. Other samples, with much larger hysteresis, show field increasing curves which are nearly the same as for this sample, but the field decreasing curves are much different. Hence it seems that the field increasing curve is a more fundamental characteristic which does not change from sample to sample. The field decreasing curve, on the other hand, changes substantially from sample to sample and approaches the field increasing curve as the irreversibility is eliminated. Values of the thermodynamic critical field H_c determined from the field increasing and field decreasing curves differ by only about 4% for this best sample.

A more detailed view of the data for V in the region of H_{c1} is shown in Fig. 4. Here both $\bar{B}$ and

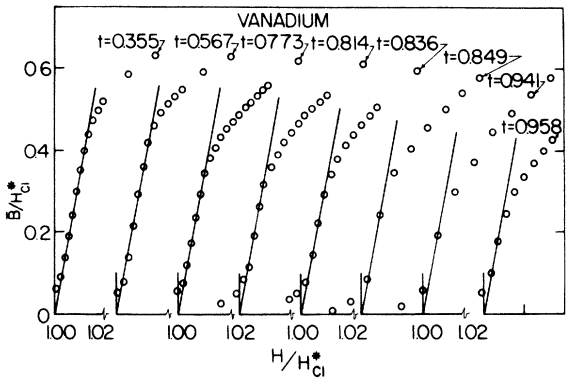

FIG. 4. Expanded view of the phase transition at H_{c1} for V. All the solid lines have the same slope of 26 G/Oe.

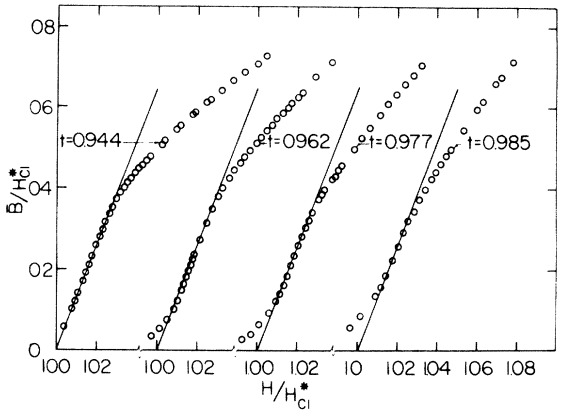

FIG. 5. Expanded view of the phase transition of H_{c1} for Nb very close to T_c. All the solid lines have the same slope of 14 G/Oe.

H are normalized by H^*_{c1} and plotted on an expanded scale to emphasize the similarity of the curves. Note that the abscissa for each curve has been shifted for clarity. At low temperatures there is a long region where the $\bar{B}$ vs H curves rise with a slope of 26 G/Oe, shown by the solid lines on the each of the curves of Fig. 4. As the temperature increases, the sample continues to show a region with a slope of 26 G/Oe all the way up to temperatures above $t = T/T_c = 0.95$ but the value of $\bar{B}$ at which the data break away from this slope decreases somewhat as T approaches T_c.

For the case of Nb, the $\bar{B}$ vs H curves for both the anodized and the unanodized samples are very similar to data published previously,[12] even though the data were taken by a field-stepping rather than by a sample-motion technique. These data differ in that they represent an extension to higher temperatures. As shown by the expanded view of Fig. 5, $\bar{B}$ rises abruptly at H_{c1} with a slope of 14 G/Oe and then bends away to a smaller slope. Note that only temperatures very close to T_c are shown in Fig. 5, whereas a broader range of temperatures is shown in Fig. 4. The rounding at the low-field end of the transition is very sensitive to the proximity of the pickup coils to the end of the sample, and it can be dramatically reduced by moving the pickup coil toward the center of the sample. As noted for V, the $\bar{B}$ vs H curves rise with the same slope for all temperatures up to 98% of T_c, but the breakaway point decreases somewhat as T increases.

A determination of B_0, the value of $\bar{B}$ for which the fluxoid lattice just fills the sample, from the $\bar{B}$ vs H curve requires an understanding of the detailed shape of the curve. If $\bar{B}$ were to rise with a slope given by the geometrical demagnetizing factor, then B_0 would be the value of $\bar{B}$ where the curves break away from this slope. Indeed, if one identifies B_0 as the point where the induction breaks away from the linear region, then one obtains values which agree roughly with the value determined from the decoration technique[2] and the neutron diffraction[3] measurements. This comparison, however, can only be made to an accuracy of about 20%, because B_0 depends somewhat on mean free path. Probably a more satisfactory way to determine B_0 is to assume that the shape of the $\bar{B}$ vs H curves is governed by bulk pinning and to fit the data to the theoretical model described earlier.

These fits are shown in Fig. 6(a) and 6(b). For the V sample [Fig. 6(a)] there are only a few data points in the steeply rising region so the data have been fitted to Eq. (1) using a desk calculator. Trial values of H^*_{c1} and H_p were chosen and μ_0' was determined from the slope of the data at H_p for a series of curves. The fit converged rather rapidly. For the Nb sample [Fig. 6(b)] a computer was used to find values of H^*_{c1} and H_p which gave the smallest root-mean-square deviation of the data from Eq.

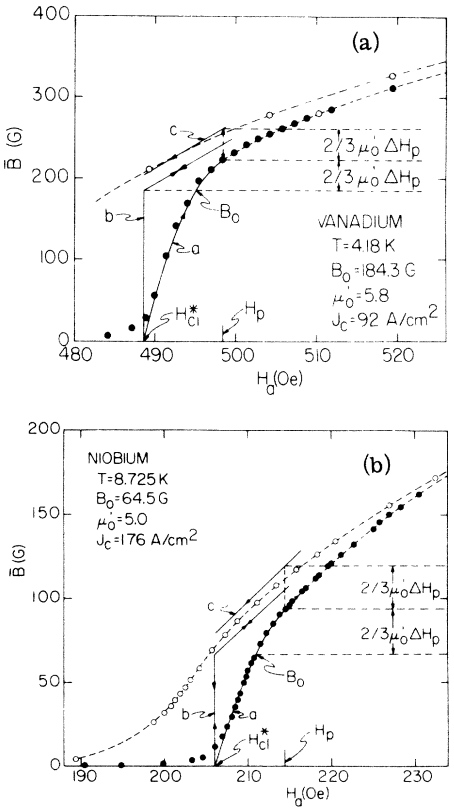

FIG. 6. Fit of the phase transitions at H^*_{c1} to the bulk-pinning critical-state model for (a) V and (b) Nb. The best-fit B_0 values occur at about the point where data deviate from linearity. Critical depinning currents J_c are proportional to H^*_{c1}. The hysteresis is close to $\Delta\bar{B}_p = 2\mu_0'\Delta H_p/3$.

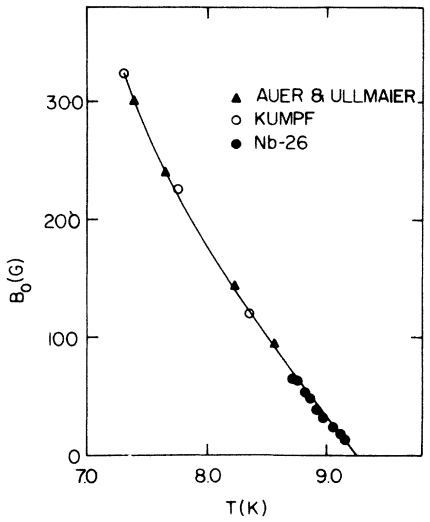

FIG. 7. Comparison of B_0 values near T_c for Nb with previously published data at lower temperatures.

(1). B_0 values determined from these procedures, indicated by the arrows on Fig. 6(a) and 6(b) are very close to the point where there is a marked deviation from the 26 G/Oe or the 14 G/Oe lines shown by the dashed curves. Hence the pinning-model interpretation gives roughly the same result as the interpretation which identifies the break from linear behavior as B_0.

An important feature of fitting the data to this pinning model is that $\Delta H_p = H_p - H_{c1}^*$ is found to be very closely proportional to H_{c1}^*. This is another way of observing that the slope is constant independent of temperature. Because ΔH_p is also proportional to the critical depinning current ($\Delta H_p = 4\pi J_c R/C$), this implies that $J_c(B_0)$ is proportional to H_{c1}^* with a proportionality constant of 7.3 A/cm^2 Oe for V and 21 A/cm^2 Oe for Nb.

Additional evidence that the bulk-pinning model applies to these data comes from the hysteresis results. A fit of the field increasing data (curves a of Fig. 6) to the pinning model determines all the parameters, H_{c1}^*, H_p, ΔH_p, and μ_0' and from these the model predicts a hysteresis of $\Delta B_p = 2\mu_0'\Delta H_p/3$. As shown in Fig. 6 this is rather close to the observed value. For V [Fig. 6(a)] the data agree with this prediction within experimental error. For Nb [Fig. 6(b)] the data are about 20% lower than the model prediction, but this is still rather good agreement. Hence bulk pinning seems to be the dominant factor controlling the shape of the transition at H_{c1}.

Values of B_0 for the Nb derived from the bulk-pinning model are in rather good agreement with the previous measurements at lower temperatures by Kumpf[4] and by Auer and Ullmaier.[10] As shown in Fig. 7, data for the anodized sample (solid circles) are a few percent below an extrapolation of the earlier data from higher temperatures (solid line), but this difference is within expected variation from sample to sample. The important aspect of Fig. 7 is that B_0 as defined here extrapolates to zero at a temperature above $0.95T_c$. Hence if we have interpreted the induction curves correctly, the lattice spacing diverges at some temperature above $0.95T_c$, and within the accuracy of these measurements, it could diverge at T_c.

A summary of the B_0 values for both samples is shown in Fig. 8 along with earlier results from Nb by Auer and Ullmaier[10] and by Kumpf.[4] B_0/H_{c1} is plotted to emphasize the manner in which B_0 goes to zero. The Nb data (solid circles) join well with the work at lower temperatures (solid dashed lines) and seem to indicate that B_0 remains finite at temperatures above $t = 0.96$. The V data are surprisingly close to the Nb data and within the accuracy of these measurements there is no difference between the behavior of Nb and V. There is, however, a large discrepancy between this V sample which has $\kappa = 0.82 \pm 0.02$ and a Ta-N sample with $\kappa = 0.845$ reported by Auer and Ullmaier.[10] B_0/H_{c1} for Ta-N goes to zero at a reduced temperature of about 0.9, whereas B_0/H_{c1} remains finite to temperatures above $0.95T_c$. Hence the temperature dependence of λ and ξ in the long-mean-free-path cases of Nb and V is rather different from the short-mean-free-path case of Ta-N alloys.

SUMMARY

Very small amounts of bulk pinning can broaden the first-order phase transition at the lower critical field and obscure the expected discontinuous rise in magnetic induction. For the Nb and V samples reported here, the shape of the magnetic induction curves for increasing applied field agrees well with the bulk-pinning model and, in addition, the magnitude of the hysteresis is close to the

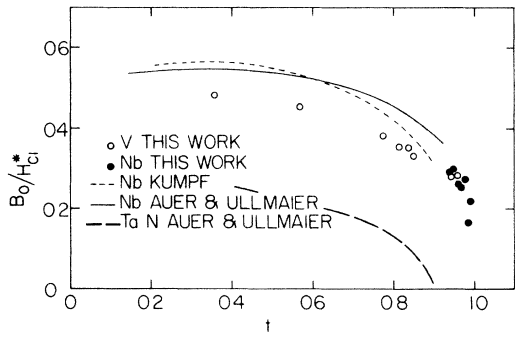

FIG. 8. Comparison of B_0/H_{c1} data for V and Nb as T approaches T_c. Neither V or Nb appear to approach zero at T less than T_c as in the case for Ta-N alloys (Ref. 10).

model prediction of $\Delta B_p = 2\mu_0'\Delta H_p/3$. Values of B_0 calculated from the data by this pinning model show that the transition from an attractive to a repulsive interaction between vortices in the long mean-free-path intrinsic type-II superconductors, Nb and V, occurs at temperatures above $t = 0.95$. A word of caution, however, is in order. The broadening of the transition by pinning prevents a direct observation of the first-order transition and makes an evaluation of B_0 from the data difficult. In fact, one cannot say with certainty that the phase transition is first order at any temperature.

ACKNOWLEDGMENTS

We would like to thank F. A. Schmidt for the preparation of the vanadium sample and J. R. Hopkins for the preparation of the Nb sample. O. D. McMasters performed some of the x-ray crystal-structure determinations.

---

*Present address: Air Force Material Laboratory/LPE Wright Patterson Air Force Base, Dayton, Ohio.

[1]A. Seeger, Comments Solid State Phys. 3, 97 (1970).
[2]V. Essmann, Phys. Lett. A 41, 477 (1972).
[3]J. Schelten, H. Ullmaier, and W. Schmatz, Phys. Status Solidi 48, 619 (1971); J. Schelten, H. Ullmaier, and G. Lippman, Z. Phys. 253, 219 (1972).
[4]V. Kumpf, Phys. Status Solidi B 44, 829 (1971).
[5]M. C. Leung, J. Low Temp. Phys. 12, 215 (1973); M. C. Leung and A. E. Jacobs *ibid.* 11, 395 (1973).
[6]L. Kramer, Z. Phys. 258, 367 (1973).
[7]A. E. Jacobs, Phys. Rev. B 4, 3029 (1971).
[8]P. G. deGennes, *Superconductivity of Metals and Alloys* (Benjamin, New York, 1966), p. 83.
[9]K. Dichtel, Phys. Lett. A 35, 285 (1971).
[10]J. Auer and H. Ullmaier, Phys. Rev. B 7, 136 (1973).
[11]V. Essmann, in *Proceedings of the International Conference on the Science of Superconductivity*, edited by F. Chilton (North-Holland, Amsterdam, 1971).
[12]D. K. Finnemore, T. F. Stromberg, and C. A. Swenson, Phys. Rev. 149, 231 (1966); D. K. Finnemore, J. R. Clem, and T. F. Stromberg, Phys. Rev. B 6, 1056 (1972).
[13]R. A. French, Cryogenics 5, 52 (1967).
[14]D. K. Finnemore and D. E. Mapother, Phys. Rev. 507, A518 (1965).
[15]Y. B. Kim and M. J. Stephen, in *Superconductivity*, edited by R. D. Parks (Marcel Dekker, New York, 1969), p. 1107.
[16]O. N. Carlson, F. A. Schmidt, and D. G. Alexander, Met. Trans. 3, 1249 (1972).
[17]J. R. Hopkins and D. K. Finnemore, Phys. Rev. B 8, (1974).
[18]F. G. Brickwedde, H. van Dijk, M. Durieux, J. R. Clement, and J. K. Logan, J. Res. Natl. Bur. Std. A 64, 1 (1960).
[19]D. K. Finnemore, J. E. Ostenson, and T. F. Stromberg, USAEC Report No. IS-1046, 1964 (unpublished).
[20]J. F. Cochran, D. E. Mapother, and R. E. Mould, Phys. Rev. 103, 1657 (1956).